RSC Advances

PAPER

View Article Online
View Journal | View Issue

Open Access Article. Published on 17 January 2017. Downloaded on 7/16/2025 12:56:44 AM.
This article is licensed under a Creative Commons Attribution 3.0 Unported Licence.

Cite this: *RSC Adv.*, 2017, **7**, 5549

A hydrophilicity-based fluorescent strategy to differentiate cysteine/homocysteine over glutathione both *in vivo* and *in vitro*†

Xiaoman Peng,‡[a] Hua Yuan,‡[a] Jian Xu,[a] Fengxian Lu,[a] Liangqian Wang,[a] Xudong Guo,[a] Shuangqing Wang,[a] Shayu Li,*[a] Yi Li*[b] and Guoqiang Yang*[a]

Received 21st November 2016
Accepted 26th December 2016

DOI: 10.1039/c6ra27074c

www.rsc.org/advances

An easily-prepared probe/nanogel composite indicator HTBNM/PU was presented, which showed selective fluorescence responses to cysteine/homocysteine over glutathione both *in vivo* and *in vitro* based on the different hydrophilicity of these biothiols. In principle, this approach could endow any lipophilic thiol indicator with selectivity for sulfur-containing amino acids.

Cysteine (Cys) and homocysteine (Hcy) as the only sulfur-containing amino acids have been proven to possess several significant biological functions.[1–3] These monothiols are involved directly in the formation of the high energy molecule acetyl-CoA, essential nutrient taurine and a variety of iron-sulfur proteins in providing the sulfur element.[4] Abnormal levels of Cys/Hcy have been claimed to be associated with a wide range of diseases such as liver damage, skin lesions, and cardiovascular ailments.[5,6] A rapid and specific detection of Cys/Hcy *in vivo* is therefore considerably valuable for diagnosis and triage in the initial phase of the related diseases. In recent years, a number of indicators have been reported that are capable of detecting Cys/Hcy.[7–12] Almost all are based on the reactions of nucleophile thiol group such as Michael addition, sulfonamide/sulfonate ester cleavage and deprotection of 2,4-dinitrobenzenesulfonyl (DNBS) from fluorophore.[13–15] As a result, rare indicators can differentiate Cys/Hcy from glutathione (GSH) that the most abundant biothiol *in vivo*.[16–18]

Very recently, a few molecular strategies have been developed for designing fluorescent indicator that can selectively probe Cys/Hcy over GSH by exploiting the synergistic effect of their sulfhydryl group and the adjacent amine group,[19] which contains specific reactions such as cyclization with aldehydes,[20–23] conjugate addition–cyclization with acrylates,[24,25] native chemical ligation,[26,27] and aromatic substitution–rearrangement,[28–30] or utilizing supramolecular interactions such as hydrogen bonding and electrostatic interactions.[31–34] Although the above strategies are ingenious, the challenge to prepare practical and cost-effective Cys/Hcy indicators still remains. The specific indicators are generally synthesized with more complicated routes. A number of them could only be operated in mixed solvents due to the poor water-solubility.[35,36] Moreover, the photobleaching under continual irradiation is still a problem for most indicators.

All reported specific indicators are based on the various reactivities of Cys, Hcy and GSH, but in fact the differences between the biothiols are far more than the mentioned one. For instance, these biothiols show a different hydrophilicity even though all of them are water-soluble. Cys/Hcy have traditionally been considered to be hydrophilic amino acid, however, they have also shown some stabilize hydrophobic interactions in special occasion.[37] GSH, on the contrary, is a totally hydrophilic molecule insoluble even in methanol. The clog *P* values of Cys, Hcy and GSH in zwitterionic forms, the most probable configuration in physiological environment, are calculated as −3.29, −3.68 and −8.59, respectively. This significant difference gave us an inspiration for selective recognition of Cys/Hcy, placing hydrophobic indicators in amphiphilic region that blocks the entry of GSH. In principle, this innovative approach can endow any lipophilic thiols indicator with selectivity for Cys/Hcy. Of course, a hydrophilic but microscopic amphiphilic carrier has to be introduced to bring the hydrophobic indicator into water environment.

To test our approach, here we designed a composite system consisted of a nanogel and a nonselective thiols indicator. Nanogels have been well demonstrated as delivery carrier for water-insoluble drug due to their stable hydrophobic nanostructures.[38–40] In this work a special polyurethane (PU) nanogel with 50% water content was chosen as the carrier because of its excellent stability and biocompatibility.[41–43] With regard to

[a]*Beijing National Laboratory for Molecular Sciences, Key Laboratory of Photochemistry, Institute of Chemistry, University of Chinese Academy of Sciences, Chinese Academy of Sciences, Beijing 100190, China. E-mail: gqyang@iccas.ac.cn; shayuli@iccas.ac.cn; Fax: +86 10 82617315; Tel: +86 10 82617263*

[b]*Key Laboratory of Photochemical Conversion and Optoelectronic Materials, Technical Institute of Physics and Chemistry, Chinese Academy of Sciences, Beijing 100190, China. E-mail: yili@mail.ipc.ac.cn*

† Electronic supplementary information (ESI) available: Details synthesis and experimental procedure, additional spectra (fluorescence emission, NMR and ESI-MS). See DOI: 10.1039/c6ra27074c

‡ These authors contributed equally to this work.

Open Access Article. Published on 17 January 2017. Downloaded on 7/16/2025 12:56:44 AM.
This article is licensed under a Creative Commons Attribution 3.0 Unported Licence.

indicator, a triarylboron luminogen was functionalized non-conjugately with maleimide moiety to afford 1-(2-((4-((4-((2-hydroxyethyl)amino)naphthalen-1-yl)(2,4,6-triisopropylphenyl) boryl)naphthalen-1-yl)amino)ethyl)-1*H*-pyrrole-2,5-dione (HTBNM). Maleimide as electron acceptor is a well-known photoinduced electron transfer (PET) quencher, often used as receptor for thiols.[44,45] The fluorescent triarylboron compounds are known for their high quantum efficiency and photostability.[46–50] The nonpolar conjugated structure also endows HTBNM with strongly hydrophobic characteristic (clog P = 9.97), lowering the possible interaction with GSH. The details of the synthesis procedure and the corresponding identification data of all compounds as well as the preparation of the nanogel indicator HTBNM/PU are provided in ESI.†

The appearance of HTBNM/PU revealed by scan electron microscopy (SEM) is monodisperse spherical nanoparticles with an average size of about 40–50 nm (Fig. S1a†). The correlated *Z*-average diameter measured by dynamic light scattering (DLS) is 67 nm, which is slightly larger than the size given by the SEM image (Fig. S1b†). This particle size distribution suggests that the composite indicator is suitable for biothiol detection in various interstitial fluid and cytosol. HTBNM/PU presents very weak fluorescence ($\Phi_F = 0.001$) in phosphate buffer (10 mM, pH 7.4). If adding Cys solution, the composite indicator shows a dramatic emission enhancement (~200 fold) and the spectral shapes are completely consistent with that of luminogen 2,2′-((((2,4,6-triisopropylphenyl)boranediyl)bis(naphthalene-4,1-diyl)) bis(azanediyl))diethanol (TBNE, Fig. 1a and S2a†). This response and the MALDI-TOF MS result (Fig. S3†) demonstrate that the recognition mechanism of PET-blocked with thiols as shown in Scheme 1. Moreover, the fluorescence response of HTBNM/PU within 30 min in the absence of thiols is close to the horizontal line (Fig. 1b). And the appearances of the indicator before and after reacted with the thiol show little difference compared to each other (Fig. S1b and c†). Both phenomena indicate the well stability of the composite indicator.

The kinetic experiments of the thiols recognition were conducted by monitoring the fluorescence intensity of the indicators. Upon addition of Cys, the emission intensity increases dramatically (Fig. S4a†) in the initial 3 min and keeps equilibrate after 5 min. The similar extent is reached within 5 and 10 min treated with Hcy. The corresponding apparent reaction rate constant (k_r) for Cys and Hcy are calculated as 10.5 mol L^{-1} s^{-1} and 5.1 mol L^{-1} s^{-1}, respectively. This rapid responses promise HTBNM/PU as a candidate of good indicator for Cys/Hcy sensing. In contrast to Cys/Hcy, GSH only increases slightly the indicator emission in 5 min (Fig. 1b and S4b†). The apparent reaction rate constant (k_r) is determined as only 0.13 mol L^{-1} s^{-1}, about 80-fold smaller than that from Cys. It is worthy to note that HTBNM without encapsulating nanogel performs fast and strong emission intensity when reacted with GSH which was comparable to Cys/Hcy (Fig. S4c†). The phenomena indicates that HTBNM/PU with the protection of nanogel performs high kinetic selectivity to Cys/Hcy rather than the counterpart GSH.

Two probable reasons to explain the high specificity of HTBNM/PU to Cys/Hcy over GSH: (1) the relatively larger steric hindrance of tripeptide GSH than that of Cys/Hcy may reduce the opportunity of getting inside the nanogel network to react with maleimide moieties; (2) as mentioned above, GSH with ultrahigh hydrophilicity, especially in its zwitterionic form, only enters into the hydrophilic domains of nanogels and hardly reacts with HTBNM encapsulated in the hydrophobic region. The first reason is obvious and self-evident. The second one is based on the heterogeneous structure of nanogels, the aqueous cavities and the amphiphilic polymer backbone.[51,52] GSH cannot be expected to diffuse in the hydrophobic region of the nanogel due to its strong lipophilicity and higher molecular weight.[53]

To further understand the second reason, we used sodium 2-mercaptoethanesulfonate (MESNa) and glutathione reduced ethyl ester (GSH-Et, the esterificated GSH, Fig. S2b†) as reference analytes. MESNa, with smaller volume than Cys/Hcy, only enhances moderately the indicator emission (Fig. 1b). The relatively low rate constant (k_r = 1.8 mol L^{-1} s^{-1}) originates

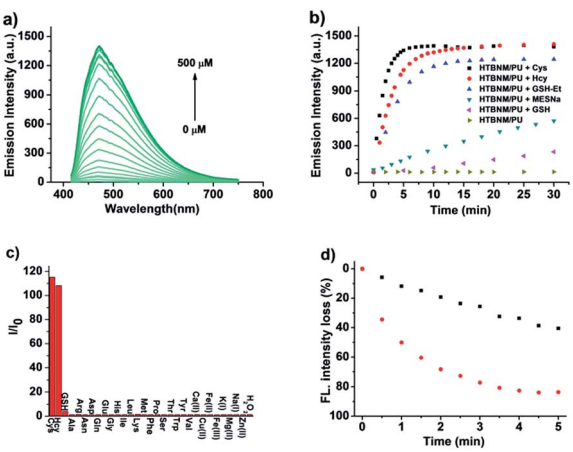

Fig. 1 (a) Fluorescence spectral changes of HTBNM/PU (2.0 μM) upon addition of Cys (0 to 500 μM) in phosphate buffer (10 mM, pH 7.4) at 37 °C. Excitation wavelength was 405 nm, so did other experiments without extra explanation. (b) Time-dependent emission intensity (at 470 nm) of HTBNM/PU towards biothiols (1.0 mM Cys, Hcy, GSH-Et, MESNa and GSH) in phosphate buffer at 37 °C. (c) Fluorescence responses of probe HTBNM/PU towards different analytes (1.0 mM), all data were acquired after addition biospecies 10 minutes. (d) Fluorescence intensity loss (%) of HTBNM in PU nanogels (black) and THF (red) upon addition of Cys (1.0 mM, pH 7.4) with increasing doses of UV (365 nm) exposure.

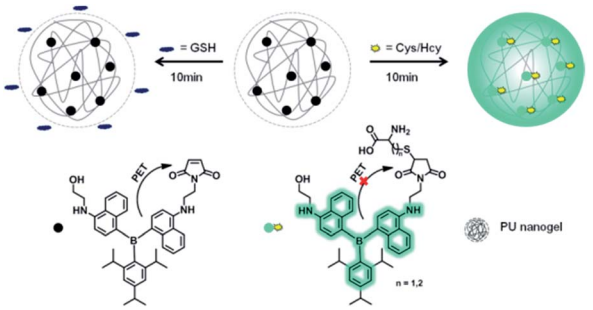

Scheme 1 Mechanism of HTBNM/PU for selective detection of Cys/Hcy over GSH.

This journal is © The Royal Society of Chemistry 2017

Open Access Article. Published on 17 January 2017. Downloaded on 7/16/2025 12:56:44 AM.
This article is licensed under a Creative Commons Attribution 3.0 Unported Licence.

apparently from the higher hydrophilicity (clog $P = -4.41$). GSH-Et possesses more hydrophobicity compared to GSH, which makes it easier to penetrate into the hydrophobic environment. It is found that HTBNM/PU performs a considerable emission enhancement upon the addition of GSH-Et (Fig. 1b). The relatively lower reactivity ($k_r = 3.0$ mol L^{-1} s^{-1}) compared to Cys/Hcy could be attributed to the steric hindrance effect. Meanwhile, the polarity in the nanogel, measured by the pyrene I_3/I_1 method, is very close to ethylene glycol which is a poor solvent for GSH (Fig. S5†).[54] The above results demonstrate clearly that molecular hydrophilicity is the most likely reason for the specific detection, although the steric hindrance effect is also remarkable.

A reliable fluorescent indicator, especially for *in vivo* attempts, selectivity, photostability and biocompatibility are three most important performances to be evaluated. In this work the response characteristics of the indicator for several non-thiol biospecies were examined in phosphorous buffer. As can be seen from Fig. 1c, only slight fluorescence changes are observed, indicating the excellent selectivity for Cys/Hcy. We compared the photostability of the composite indicator with that of HTBNM in THF solution. Although the fluorescence intensity of both systems decreases with growing doses of UV exposure, the experimental results clearly demonstrate that the nanogel carrier considerably enhances the photostability of HTBNM (Fig. 1d). The cytotoxicity of HTBNM/PU on NIH/3T3 fibroblasts (obtained from China Infrastructure of Cell Line Resources (Beijing Headquarters) for Cell Ordering Service) is determined by the standard 3-(4,5-dimethyl-2-thiazolyl)-2,5-diphenyltetrazolium bromide (MTT) assay. The MTT results show that the cell viability is not obviously affected by the composite even when the HTBNM concentration is as high as 5.0 μM (Fig. S6†).

We introduced HTBNM/PU in cultured NIH/3T3 fibroblasts to explore its utility for *in vivo* Cys/Hcy imaging. As emphasized above, HTBNM/PU is nonemissive before treated with thiols. Thus, the conventional washing of free indicator is not necessary, prompt imaging is feasible. Initial experiment that NIH/3T3 incubated with the composite (HTBNM, 1.0 μM) for 10 min reveals significant fluorescence in green channel (Fig. 2a). Detailed fluorescence images show that the indicators are localized all over the cytosol, confirming the admirable permeability of HTBNM/PU. The pre-addition of *N*-ethylmaleimide (NEM, 0.5 mM), a known thiol-blocking agent, to the cell culture leads to very weak fluorescence (Fig. 2b), indicating that the fluorescence is directly responsive to endogenous thiols. To differentiate which thiol induces the turn-on fluorescence, NIH/3T3 cells were pretreated with Cys and GSH, respectively. The Cys treated cells show a remarkable fluorescent enhancement compared to untreat ones (Fig. 2c). In stark contrast, no notable changes of green emission are observed in GSH pretreated cells (Fig. 2d). These *in vivo* results show clearly the specificity of HTBNM/PU for Cys over GSH. In addition, we noted that HTBNM/PU presents a good photostability in living cells (Fig. S7†).

Encouraged by the results of above exogenous biothiols adjustment, we were interested in applying the HTBNM/PU to monitoring the real process involving Cys/Hcy changes. GSH is known as the most efficient antioxidant that protects cells from oxidative stress caused by reactive oxygen species (ROS),[55,56] however, the role of Cys/Hcy in reduction of ROS is not very clear. In principle, Cys/Hcy and GSH should show a similar reactive behavior that covalent bonding to other biothiols to form disulfide bonds.[57] To *in situ* observe the interaction of Cys/Hcy and ROS, the NIH/3T3 fibroblasts were challenged with H_2O_2, the major ROS species.[58–60] It is obvious that intracellular fluorescence intensity declines with increasing H_2O_2 treated time (Fig. 3), suggesting the decreased intracellular Cys/Hcy levels under H_2O_2-induced oxidative stress. The above results clearly indicate that Cys/Hcy are also involved in the resistance to oxidation. The visible response of Cys/Hcy for ROS demonstrates the capability of the composite indicator.

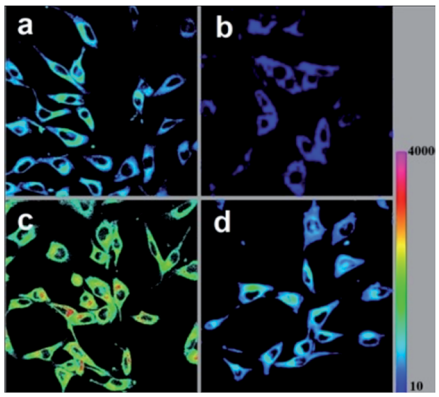

Fig. 2 Confocal fluorescence images of NIH/3T3 fibroblasts: (a) incubated with HTBNM/PU (2.0 μM) for 10 min; (b) pretreated with 0.5 mM NEM for 30 min and then incubated with HTBNM/PU; (c) pretreated with 0.5 mM Cys for 30 min and then incubated with HTBNM/PU; (d) pretreated with 0.5 mM GSH for 30 min and then incubated with HTBNM/PU. The intensity data were collected at 450–500 nm.

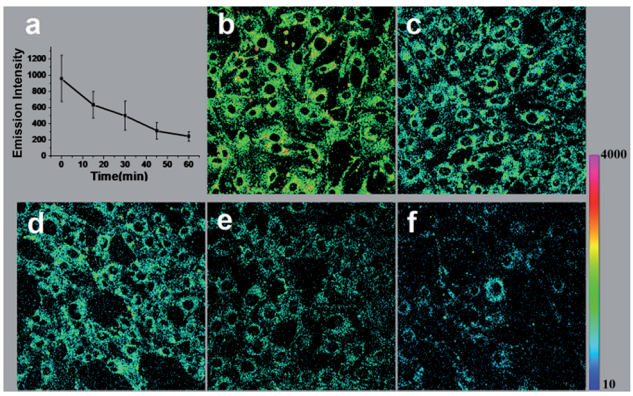

Fig. 3 (a) Time course of fluorescence intensity of NIH/3T3 fibroblasts treated by H_2O_2. Monitoring of Cys levels of NIH/3T3 fibroblasts. (b), (c), (d), (e) and (f) Confocal fluorescence images of NIH/3T3 fibroblasts pretreated with 1 mM H_2O_2 for 0 min, 15 min, 30 min, 45 min, 60 min, respectively, and then incubated with HTBNM/PU. The intensity data were collected at 450–500 nm.

Open Access Article. Published on 17 January 2017. Downloaded on 7/16/2025 12:56:44 AM.
This article is licensed under a Creative Commons Attribution 3.0 Unported Licence.

Conclusions

In summary, we have demonstrated a novel approach to differentiate Cys/Hcy over GSH based on the different hydrophilicity of these biothiols, where the developed example indicator combined triarylboron compound with PU nanogels shows excellent specificity both *in vivo* and *in vitro*. This approach is universal and can be extended to any other unselective indicators, which overcomes several limitations imposed by synthesis approaches. This represents the first use of a physical rather than a chemical process for improving selectivity. It is impressed that both biocompatibility and photostability are simultaneously improved by the nanogels. We expect that the simplicity and efficiency of this approach will further stimulate the integration of composite indicators into both chemical and biologic sensing field.

Acknowledgements

We are grateful for funding from the National Basic Research Program (2013CB834505, 2013CB834703, 2011CBA00905, and 2009CB930802) and the National Natural Science Foundation of China (Grant No. 21273252, 21072196, 21233011, and 21205122).

References

1 X. Chen, Y. Zhou, X. Peng and J. Yoon, *Chem. Soc. Rev.*, 2010, **39**, 2120.
2 E. Weerapana, C. Wang, G. M. Simon, F. Richter, S. Khare, M. B. D. Dillon, D. A. Bachovchin, K. Mowen, D. Baker and B. F. Cravatt, *Nature*, 2010, **468**, 790.
3 C. Yin, F. Huo, J. Zhang, R. Martinez-Manez, Y. Yang, H. Lv and S. Li, *Chem. Soc. Rev.*, 2013, **42**, 6032.
4 H. S. Jung, X. Chen, J. S. Kim and J. Yoon, *Chem. Soc. Rev.*, 2013, **42**, 6019.
5 S.-Q. Wang, Q.-H. Wu, H.-Y. Wang, X.-X. Zheng, S.-L. Shen, Y.-R. Zhang, J.-Y. Miao and B.-X. Zhao, *Analyst*, 2013, **138**, 7169.
6 R. Peng, L. Lin, X. Wu, X. Liu and X. Feng, *J. Org. Chem.*, 2013, **78**, 11602.
7 J. Xu, H. Yu, Y. Hu, M. Chen and S. Shao, *Biosens. Bioelectron.*, 2016, **75**, 1.
8 K. Yin, F. Yu, W. Zhang and L. Chen, *Biosens. Bioelectron.*, 2015, **74**, 156.
9 M.-Y. Jia, L.-Y. Niu, Y. Zhang, Q.-Z. Yang, C.-H. Tung, Y.-F. Guan and L. Feng, *ACS Appl. Mater. Interfaces*, 2015, **7**, 5907.
10 N. Shao, J. Y. Jin, S. M. Cheung, R. H. Yang, W. H. Chan and T. Mo, *Angew. Chem., Int. Ed.*, 2006, **45**, 4944.
11 H. T. Zhang, R. C. Liu, J. Liu, L. Li, P. Wang, S. Q. Yao, Z. T. Xu and H. Y. Sun, *Chem. Sci.*, 2016, **7**, 256.
12 L.-Y. Niu, Q.-Q. Yang, H.-R. Zheng, Y.-Z. Chen, L.-Z. Wu, C.-H. Tung and Q.-Z. Yang, *RSC Adv.*, 2015, **5**, 3959.
13 Y. Zeng, G. Zhang and D. Zhang, *Anal. Chim. Acta*, 2008, **627**, 254.
14 F.-J. Huo, Y.-Q. Sun, J. Su, J.-B. Chao, H.-J. Zhi and C.-X. Yin, *Org. Lett.*, 2009, **11**, 4918.
15 S.-M. Ji, H.-M. Guo, X.-L. Yuan, X.-H. Li, H.-D. Ding, P. Gao, C.-X. Zhao, W.-T. Wu, W.-H. Wu and J.-Z. Zhao, *Org. Lett.*, 2010, **12**, 2876.
16 J. Pan, Y. Zhang, J. Xu, J. Liu, L. Zeng and G.-M. Bao, *RSC Adv.*, 2015, **5**, 97781.
17 X. Zhu, Y. Li, W. Zan, J. Zhang, Z. Chen, X. Liu, F. Qi, X. Yao, X. Zhang and H. Zhang, *Photochem. Photobiol. Sci.*, 2016, **15**, 412.
18 S. Resa, A. Orte, D. Miguel, J. M. Paredes, V. Puente-Muñoz, R. Salto, M. D. Giron, M. J. Ruedas-Rama, J. M. Cuerva, J. M. Alvarez-Pez and L. Crovetto, *Chem.–Eur. J.*, 2015, **21**, 14772.
19 L.-Y. Niu, Y.-Z. Chen, H.-R. Zheng, L.-Z. Wu, C.-H. Tung and Q.-Z. Yang, *Chem. Soc. Rev.*, 2015, **44**, 6143.
20 P. Wang, J. Liu, X. Lv, Y. Liu, Y. Zhao and W. Guo, *Org. Lett.*, 2012, **14**, 520.
21 K.-S. Lee, T.-K. Kim, J. H. Lee, H.-J. Kim and J.-I. Hong, *Chem. Commun.*, 2008, **46**, 6173.
22 W. Lin, L. Long, L. Yuan, Z. Cao, B. Chen and W. Tan, *Org. Lett.*, 2008, **10**, 5577.
23 O. Rusin, N. N. S. Luce, R. A. Agbaria, J. O. Escobedo, S. Jiang, I. M. Warner, F. B. Dawan, K. Lian and R. M. Strongin, *J. Am. Chem. Soc.*, 2004, **126**, 438.
24 X. Yang, Y. Guo and R. M. Strongin, *Angew. Chem., Int. Ed.*, 2011, **50**, 10690.
25 B. Liu, J. Wang, G. Zhang, R. Bai and Y. Pang, *ACS Appl. Mater. Interfaces*, 2014, **6**, 4402.
26 L. Long, W. Lin, B. Chen, W. Gao and L. Yuan, *Chem. Commun.*, 2011, **47**, 893.
27 L. Yuan, W. Lin, Y. Xie, S. Zhu and S. Zhao, *Chem.–Eur. J.*, 2012, **18**, 14520.
28 L.-Y. Niu, Y.-S. Guan, Y.-Z. Chen, L.-Z. Wu, C.-H. Tung and Q.-Z. Yang, *J. Am. Chem. Soc.*, 2012, **134**, 18928.
29 D. Kand, T. Saha and P. Talukdar, *Sens. Actuators, B*, 2014, **196**, 440.
30 L.-Y. Niu, Y.-S. Guan, Y.-Z. Chen, L.-Z. Wu, C.-H. Tung and Q.-Z. Yang, *Chem. Commun.*, 2013, **49**, 1294.
31 N. Shao, J. Jin, H. Wang, J. Zheng, R. Yang, W. Chan and Z. Abliz, *J. Am. Chem. Soc.*, 2010, **132**, 725.
32 X. Zhou, X. Jin, G. Sun, D. Li and X. Wu, *Chem. Commun.*, 2012, **48**, 8793.
33 J. Liu, Y.-Q. Sun, H. Zhang, Y. Huo, Y. Shi, H. Shi and W. Guo, *RSC Adv.*, 2014, **4**, 64542.
34 M. Işık, R. Guliyev, S. Kolemen, Y. Altay, B. Senturk, T. Tekinay and E. U. Akkaya, *Org. Lett.*, 2014, **16**, 3260.
35 H. Liu, X. Wang, Y. Xiang and A. Tong, *Anal. Methods*, 2015, **7**, 5028.
36 Y. Yue, C. Yin, F. Huo, J. Chao and Y. Zhang, *Sens. Actuators, B*, 2016, **223**, 496.
37 A. Bargellesi, S. Pontremoli, C. Menini and F. Conconi, *Eur. J. Biochem.*, 1968, **3**, 364.
38 M. Oishi and Y. Nagasaki, *Nanomedicine*, 2010, **5**, 451.
39 H. Koo, M. S. Huh, J. H. Ryu, D.-E. Lee, I.-C. Sun, K. Choi, K. Kim and I. C. Kwon, *Nano Today*, 2011, **6**, 204.
40 R. T. Chacko, J. Ventura, J. Zhuang and S. Thayumanavan, *Adv. Drug Delivery Rev.*, 2012, **64**, 836.

 This journal is © The Royal Society of Chemistry 2017

Open Access Article. Published on 17 January 2017. Downloaded on 7/16/2025 12:56:44 AM.
This article is licensed under a Creative Commons Attribution 3.0 Unported Licence.

41 T. Jokic, S. M. Borisov, R. Saf, D. A. Nielsen, M. Kühl and I. Klimant, *Anal. Chem.*, 2012, **84**, 6723.
42 H.-s. Peng, J. A. Stolwijk, L.-N. Sun, J. Wegener and O. S. Wolfbeis, *Angew. Chem., Int. Ed.*, 2010, **49**, 4246.
43 L. Cao, X. Li, S. Wang, S. Li, Y. Li and G. Yang, *Chem. Commun.*, 2014, **50**, 8787.
44 X. Guo, X. Zhang, S. Wang, S. Li, R. Hu, Y. Li and G. Yang, *Anal. Chim. Acta*, 2015, **869**, 81.
45 Y. Yang, F. Huo, C. Yin, J. Chao and Y. Zhang, *Dyes Pigm.*, 2015, **114**, 105.
46 X. Li, X. Guo, L. Cao, Z. Xun, S. Wang, S. Li and G. Yang, *Angew. Chem., Int. Ed.*, 2014, **53**, 7809.
47 J. Feng, L. Xiong, S. Wang, S. Li, Y. Li and G. Yang, *Adv. Funct. Mater.*, 2013, **23**, 340.
48 P. Chen, R. A. Lalancette and F. Jäkle, *Angew. Chem., Int. Ed.*, 2012, **51**, 7994.
49 A. K. C. Mengel, B. He and O. S. Wenger, *J. Org. Chem.*, 2012, **77**, 6545.
50 H. Li, R. A. Lalancette and F. Jakle, *Chem. Commun.*, 2011, **47**, 9378.
51 B. Rossi, V. Venuti, F. D'Amico, A. Gessini, A. Mele, C. Punta, L. Melone, V. Crupi, D. Majolino, F. Trotta and C. Masciovecchio, *Soft Matter*, 2015, **11**, 5862.
52 B. Rossi, V. Venuti, F. D'Amico, A. Gessini, F. Castiglione, A. Mele, C. Punta, L. Melone, V. Crupi, D. Majolino, F. Trotta and C. Masciovecchio, *Phys. Chem. Chem. Phys.*, 2015, **17**, 963.
53 C. A. Lipinski, F. Lombardo, B. W. Dominy and P. J. Feeney, *Adv. Drug Delivery Rev.*, 1997, **23**, 3.
54 K. Kalyanasundaram and J. K. Thomas, *J. Am. Chem. Soc.*, 1977, **99**, 2039.
55 Y. Zhang, X. Shao, Y. Wang, F. Pan, R. Kang, F. Peng, Z. Huang, W. Zhang and W. Zhao, *Chem. Commun.*, 2015, **51**, 4245.
56 X.-F. Yang, Q. Huang, Y. Zhong, Z. Li, H. Li, M. Lowry, J.-O. Escobedo and R.-M. Strongin, *Chem. Sci.*, 2014, **5**, 2177.
57 W. Dröge, *Philos. Trans. R. Soc., B*, 2005, **360**, 2355.
58 B. V. Chernyak, D. S. Izyumov, K. G. Lyamzaev, A. A. Pashkovskaya, O. Y. Pletjushkina, Y. N. Antonenko, D. V. Sakharov, K. W. Wirtiz and V. P. Skulachev, *Biochim. Biophys. Acta*, 2006, **1757**, 525.
59 M. Zheng, H. Huang, M. Zhou, Y. Wang, Y. Zhang, D. Ye and H. Y. Chen, *Chem.–Eur. J.*, 2015, **21**, 10506.
60 R. S. Bhimani, W. Troll, D. Grunberger and K. Frenkel, *Cancer Res.*, 1993, **53**, 4528.